



## A Mixed Sub/Super Critical Flow Solver for Multiple Slope Canals

Mahyar Mohamadzadeh<sup>1</sup>, Qomi, Saeed Reza Sabbagh Yazdi<sup>2</sup>, Asghar Bohluly<sup>3</sup>

1,3- MSc., NAMROOD Riverine & Coastal Environment

2- PhD, KNT University of Technology

Mohamadzadeh@namrood.com

### Abstract

This paper introduces a numerical method for solving free surface flow in canals with bed slopes. The model is suitable for computation of flow velocity pattern and water depths. The developed numerical algorithm solves the set of shallow water equations. The set of equations contains the continuity and motion equations in horizontal plane. The effect of bed slope is included in the gravitational term of the equations of motion, while the effects of bed and wall frictions considered in the global stresses. The governing equations were converted to discrete form on unstructured mesh using the cell vertex finite volume method. The developed model is utilized for flow simulation in a number of flow regimes in prismatic canals, which have two different constant bed slope parts. The numerical results present the ability of the model to simulate super-critical flow, sub-critical flow and mixed flow in canals according to the combination of bed slopes. The accuracy of the results is assessed by comparison of computed results with the analytical solutions.

**Keywords:** Shallow Water Equations, Finite Volume Method, Unstructured Grid, Multiple Bed Slope

### Introduction

The shallow water equations have a wide application for solving many types of two dimensional real world flow problems such as internal flows, atmospheric flows, coastal flows, tidal flows, tidal mixing, residual currents, storm surges, river flows, dam-break waves, lake flows, and planetary flows. The main assumptions for using shallow water equation is hydrostatic distribution of pressure, which means there is no significant velocity component in vertical direction and uniform distribution of horizontal velocity in vertical plane. However, the classic shallow water equations assume the channel bed is horizontal [1]. Therefore, the classic shallow water equation is not able to simulate flows in cases with complex topography while this situation exists in wide range of real cases. Therefore, considering bed slope and topography variations of the case improve ability of the shallow water equations to simulate real applications. By considering the channel bed in the shallow water equations, one may simulate supercritical flow (i.e. in chute spillways). The bed slope of the channel is mathematically modeled in four different ways in the equations of the motions. First, for the mild and constant channel bed, the effect of bed slope can be considered as a global force in the sink/source terms as a constant value. This scheme is applicable for limited range of real cases. Second, computing bed slope via adding a spatially variable term as a function of local slopes in to horizontal directions ( $-\partial z/\partial x$  and  $-\partial z/\partial y$ ) in the sink/source terms of equations of motion [1]. This scheme can be computed bed slope for wider range of real cases, but it is not applicable for the cases with the steep slopes and faces numerical difficulties in the cases with sudden variations of the bed slope. Third, the bed slope can be considered in the gravitational terms which represent the hydrostatic pressure effects (using  $-\partial(h+z)/\partial x$  and  $(-\partial(h+z)/\partial y)$ ) in the equations of motion. Applying this scheme, the shallow water equations can numerically simulate flows over irregular sloping beds with considerably less computation efforts [2]. Forth, the coordinate system of equations must be transformed to a plane, which its normal corresponds to the bed surface normal at each computational node [2]. This scheme is applicable to the cases with steep slopes but suits to cases with smooth and regular changes of bed slopes. However, the transformation of equations to the curvilinear coordinates may increase the computational complexities. In this work, a mixed of third and forth schemes of the above mathematical modeling of bed slope in the set of shallow water equations are used for numerically simulation of different flow regimes (sub-critical, super-critical, and mixed of sub and super-critical) in a long channel with dual bed slopes. It should be mentioned that in this model, super critical flows are simulated using the forth method and the third method is

---

1,3- Senior Engineer in Computational hydraulic

2- Associated professor, Faculty of Civil Engineering



applied to the model for simulating subcritical flows. Regions of each of super and sub critical flows can be defined by the user using coordinate of interface of the regions.

The cell vertex finite volume method suitable for the triangular unstructured meshes is applied to convert the mathematical equation to discrete formulations. In order to avoid the possible instabilities during explicit solution procedure of the convection-dominated equations, proper artificial viscosity terms, which preserve the accuracy of the solution, are added to the formulation. Proper numerical techniques are adopted for increasing the efficiency of the computation on unstructured meshes.

The computational results present encouraging agreements with the expected solutions. This success paves the way toward the simulations of more complicated real world problems.

### Mathematical Modeling

The set of shallow water equations is a special form of the Navier-Stokes equations while is obtained by integrating the Navier–Stokes equations from the bottom to the water surface of the channel. The important assumptions hydrostatic distribution of pressure means that there is no significant velocity component in vertical direction. Additional assumptions, like incompressibility of water flow, negligible shear wind stress in water surface and insignificant Coriolis effects due to earth rotation may provide further simplifications for particular problems of channel hydraulics. The convective form of the equations is usually applicable to free surface flow. In the applied form of the equations, the effect of bed slope is considered in the gravitational terms while bed and wall frictions are considered in the sink/source terms as global forces of the equations of motions.

The set of shallow water equations consist equation of continuity and two equations of motion in horizontal plane. The depth averaged continuity equation is derived from the mass conservation equation for free surface flow as:

$$\frac{\partial h}{\partial t} + \frac{\partial}{\partial x}(hu) + \frac{\partial}{\partial y}(hv) = 0 \quad (1)$$

Where  $t$  = time,  $x$  and  $y$  = Cartesian coordinates,  $h$  = flow depth and  $u$  and  $v$  = depth averaged velocity components.

The equations of motion for free surface flow in a channel with bed slope are formed from the momentum conservation equations in two Cartesian coordinates in horizontal directions. The equation of motion in  $x$  direction is written as follow.

$$\frac{\partial}{\partial t}(hu) + \frac{\partial}{\partial x}(hu^2) + gh \frac{\partial}{\partial x}(h+z) + \frac{\partial}{\partial y}(huv) = -\frac{\tau_x}{\rho} \quad (2)$$

Similarly, the equation of motion in  $y$  direction is written as follow.

$$\frac{\partial}{\partial t}(hv) + \frac{\partial}{\partial x}(huv) + \frac{\partial}{\partial y}(hv^2) + gh \frac{\partial}{\partial x}(h+z) = -\frac{\tau_y}{\rho} \quad (3)$$

Where  $t$  = time,  $x$  and  $y$  = Cartesian coordinates,  $h$  = flow depth,  $u$  and  $v$  = depth average velocity vectors,  $z$  = bed elevation,  $g$  = gravity acceleration, and  $\tau_x/\rho$  and  $\tau_y/\rho$  are global dissipative forces which are compute using following formulas [1], [2].

$$-\frac{\tau_x}{\rho} = C_f u \sqrt{u^2 + v^2} \quad , \quad -\frac{\tau_y}{\rho} = C_f v \sqrt{u^2 + v^2} \quad (4)$$

Where,  $C_f$  represents the effective global dissipative coefficient [3], which can be formed by summing the wall frictions as well as turbulence and viscosity dissipation effects at the nodal points of the flow domain [4]. Moreover, the effect of wall friction may be considered in the coefficient  $C_f$  at the wall boundary nodes [5].

### Numerical Formulation

The partial differential equations (1), (2) and (3) can be solved on triangular unstructured meshes, which is generated applying Delaunay triangulation method [6] in a coupled manner using the algorithm developed for the compressible flow problems [7].

The cell vertex finite volume method [4] is applied for discretization of equations (1), (2), and (3). In this method, the domain is divided into triangular sub-domains (control volumes), which is formed by triangles meeting every computational node, and then the governing equations are integrated over each sub-domain  $\Omega$ .



The equations of continuity and the motions are integrated over each control volume. Application of the Green's theorem to the integrated equation in general form result is:

$$\int_{\Omega} \frac{\partial W}{\partial t} d\Omega + \oint_{\Gamma} (Fdy - Gdx) = \int_{\Omega} S d\Omega \quad (5)$$

Where  $\Omega_i$  and  $\Gamma$  are the area and boundaries of the control volume, respectively.  $W$  represents time dependent terms of (1) to (3) while,  $F$  and  $G$  represent  $x$  and  $y$  dependent in (1) to (3), respectively.  $S$  is the sink/source term of the equation. Its value equals to zero for the continuity equation and equal to global forces for two equations of motion. If nodal values of dependent variables at each triangle vertex are taken as the unknowns at the central node of the control volume  $\Omega$ , the discrete explicit form of the equation is evaluated by conversion of the boundary integral into the summation over  $m$  edges of the control volume, as

$$W^{n+1} = W^n - \frac{\Delta t^n}{\Omega_i} \left[ \sum_{j=1}^m (\bar{F}\Delta y_j - \bar{G}\Delta x_j) \right] + S^n \quad (6)$$

Where  $W^{n+1}$  is the value of  $W^n$  to be computed after  $\Delta t$ . The parameters  $\bar{F}$  and  $\bar{G}$  are the average values of the fluxes in  $x$  and  $y$  spatial derivatives in each edge at the boundary edges of the control volume [7].

### Artificial Dissipation

In the explicit solution of the convective equations where the global dissipative terms are negligible, some numerical oscillations grow particularly near the high gradient regions. These numerical noises disturb the solution procedure in the cases with small physical dissipation mechanisms. For the flow problems with gradual changes in dependent variables (flows with no shock waves), the fourth order term (Biharmonic operator) produces enough dissipations to damp out the numerical oscillations and stabilize the explicit solution procedure. However, the formulation of the artificial dissipation term should preserve the accuracy of the solution. Moreover, the formulation of this additional term must be suitable for computations using irregular node numbering of the unstructured meshes utilized in present work. The artificial dissipation operator which can be added to the aforementioned algebraic formulation, is formulated as

$$\nabla^4 W_i = \varepsilon_4 \sum_{j=1}^{N_e} \lambda_{ij} (\nabla^2 W_j - \nabla^2 W_i) \quad \text{where} \quad \nabla^2 W_i = \sum_{j=1}^{N_e} (W_j - W_i) \quad (7)$$

The scaling factor,  $\lambda_{ij}$ , is computed using the maximum nodal values of Eigen values of Jacobin matrix at the edges connected to the centre of the control volume.  $\lambda$  is evaluated as follow.

$$\lambda = |\vec{U} \cdot \hat{n}| + \sqrt{U^2 + C^2 (\Delta x^2 + \Delta y^2)} \quad (8)$$

Where  $C$  = celerity,  $\vec{U}$  = average computed velocity, and  $\hat{n}$  = normal vectors at boundary edges of control volume  $\Omega$ . The celerity is computed as follow.

$$C = \sqrt{g\bar{h}} \quad (9)$$

Where  $g$  = gravity acceleration. Depending on the sizes of grid spacing, the coefficient of the artificial dissipation term,  $\varepsilon$  should be tuned to the minimum required value ( $1/256 \leq \varepsilon \leq 3/256$ ) for the applied mesh [7].

### In and out Flow boundaries

The model can distinguish inflow and outflow boundaries automatically using normal vector and velocity vector at the boundary nodes. However, manual distinction of flow boundaries can prevent computational conflicts. Flow boundary conditions are imposed concerning type of flow in each boundary while type of the flow defines using computed Froude number for the boundary cells. Following boundary conditions are implemented for sub-critical flows [8],

- 1 At inflow boundary nodes, the components of the unique width discharge,  $hu$  and  $hv$ , are specified and the depth,  $h$ , is extrapolated from the inside domain.
- 2 At the outflow boundary nodes, the depth,  $h$ , is imposed and the velocity components,  $u$  and  $v$ , are extrapolated from the interior nodes of domain.

For super-critical flow the boundary conditions are:



- 1 At inflow boundary nodes, the components of the unique width discharge,  $hu$  and  $hv$ , and the depth,  $h$ , are imposed.
- 2 At outflow boundary nodes, the velocity components,  $u$  and  $v$ , and the depth,  $h$ , are extrapolated from the interior nodes of the domain.

In some cases, mixed flow may form in a certain channel. In these cases, at each flow boundary proper boundary condition is imposed concerning the local regime of the flow. For example, at the upstream boundary, the flow is sub-critical, and at the downstream boundary, the flow is supercritical. In such a case, the free stream velocity components (or the unique width discharge components) are imposed at the upstream boundary, and the velocity components and the depth are extrapolated at the downstream boundary. Therefore, the depth is not imposed at any boundary. In this case the critical depth, which is automatically formed by the numerical flow-solver at the position where the flow regime changes, should play the role of an internal boundary condition. Then from the point that critical depth is computed, the flow depths can form toward the upstream and downstream directions [5].

### Time Marching

The time marching of the explicit computations ( $\Delta t$ ) should be proportional to the speed of wave propagation of the applied convective equations. This speed can be computed using,  $\lambda$  the maximum Eigen values of Jacobin matrix of homogenous form of the set of governing equations. Hence, for every control volume,  $\Omega_i$  in computational domain, the time marching limit is specified as,

$$\Delta t_i = (CFL) \frac{\Omega_i}{\lambda_i} \quad (12)$$

Where, parameter  $\lambda_i$  represents the maximum nodal values of Eigen values of Jacobin matrix at the edges connected to the centre of the control volume  $i$ . The Courant-Fredrsh-Levy number (coefficient  $CFL$ ) is evaluated by the stability condition for explicit computation procedure.

Since we are dealing with unstructured meshes, the size of control volumes varies over the computational domain. Therefore, every control volume has its own time step,  $\Delta t_i$ . Hence, the speed of explicit computations is limited to the minimum  $(\Delta t)_{\min}$  in the unsteady flow field. Although the values of the time step,  $\Delta t_i$  for every control volume vary during the stages of the numerical solution, it may approach to certain values when the computations converge to the steady state conditions [9].

### Efficiency Improvements

#### Local Time Stepping

The choice of  $(\Delta t)_{\min}$  for the time marching of the numerical solution may slow down the computations. For the steady flow cases, considering  $\Delta t_i$  local time step limit associated with the control volume  $\Omega_i$  will speed up the convergence to the steady state condition [9]. However for relatively long channels, the choice of local time stepping may disturb safe propagations of flow boundary condition influences, and hence, may endanger the stability of the solution procedure values of the time step,  $\Delta t_i$  for every control volume vary during the stages of the numerical solution.

#### Multi-stage time stepping

The Courant-Fredrsh-Levy number condition is relaxed by application of a three stages Runge-Kutta time stepping technique. Therefore, maximum value of the Courant-Fredrsh-Levy number limited up to 3 ( $CFL \leq 3.0$ ) [7].

#### Residual Smoothing

Smoothing the residuals (sum of convective artificial dissipation terms) increases, the stability of the computations and speeds up converge to the steady state. In present work two iterations of the implicit residual smoothing technique is utilized [10]

#### Freezing of some computations

In order to reduce the computational expenses, the artificial dissipation operator and the global forces as well as time step limited can be computed in some certain computational stages. However, the last values of these terms



are applied to the computation. Performing residual smoothing only at similar computational stages may provide additional saving [11].

### Edge-Base algorithm

In the triangular meshes, every edge is shared at two neighboring control volumes. Hence, the computation of the part of the boundary integral of convective term associated with a certain edge may perform twice. In order to save the computational efforts, the computations is done once over the edges and then the results of the computations are added to central node of the left and right control volumes with opposite sign. Similar to the convective terms, the computations of artificial dissipation at the computational nodes are performed using the edges between two computational nodes. Therefore, of this term can be computed once for two nodes of each edge using similar technique. Note that, this algorithm requires edge-base mesh data structure, which specifies the number of two end nodes as well as the left and right nodes of all the edges in the domain. [7].

### Numerical Experiments

In order to evaluate the ability of the model to simulate free surface flow in channels with bed slope, three long channel with different types of dual slopes are selected from the literature of numerical works[5]. The rectangular cross section channel has 1.4m width. Its 52.56m length consists two parts with different bed slope. The first part is 24m and the second is 28.56m long in length. The Manning's coefficient for both bed and wall is 0.02 and the value of the turbulent dissipation is equal to bed resistance. In order, the numerical simulation the utilized unstructured mesh is refined at the vicinity of the location of changing the bed slope (Fig.1).

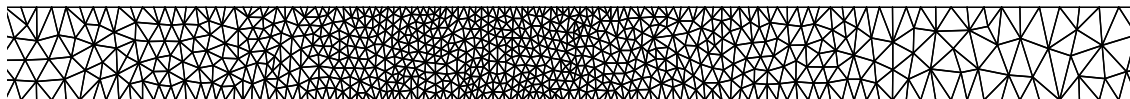


Figure 1. Unstructured mesh refined at the vicinity of the point where the bed slope changes

As the first test, both part of the channel have steep slopes ( $S_0=0.03$  and  $S_0=0.01$ ), and hence, supercritical flow is numerically simulated [5] using the fourth method of bed slope simulation. Since the flow regime is supercritical all over the channel, at the upstream boundary the depth ( $h=0.2m$ ) and the flow discharge ( $Q=0.86m^3/s$ ) are imposed [5]. The computation performed after implementation of proper initial and flow boundary conditions. As shown in figure 2, at first part of the channel, profile smooth variation of water depth is developed, but the S3 profile of the water depth in the second part uniformly formed.

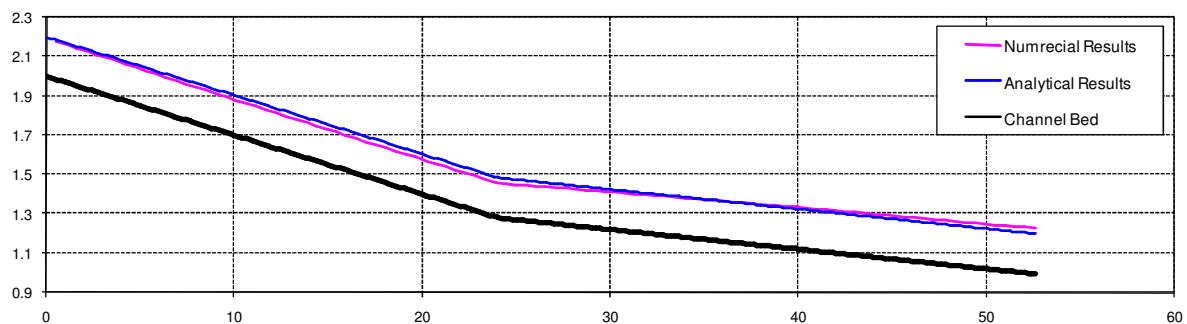


Figure 2. Water depth profile along the centerline of the channel for two steep bed slopes

In the second test, the first part of the channel has a steep slope ( $S_0=0.009$ ) while the second part of the channel has an inverse slope ( $S_0=-0.005$ ). The downstream flow depth is  $h=0.3m$  and the upstream flow discharge is reported  $Q=0.31m^3/s$  [5]. In this test, flow is sub-critical while the bed slope of the first part of the channel is steep slope and the third method of bed slope simulation utilized for this test. Due to inverse bed slope of the second part of the channel some bed resistance against flow exists and it causes increase in water depth. Increasing water depth elevates water depth in the first part of the channel. Since the flow is sub-critical, relative boundary condition is imposed at the in and out flow boundaries. In this test, constant along the channel is assumed as the initial depth (the water surface profile is parallel to the channel bed). As shown in figure 4, flat A2 water surface profile is formed in the second part while the depth variation conforms S1 profile in the first part at the end of computations.

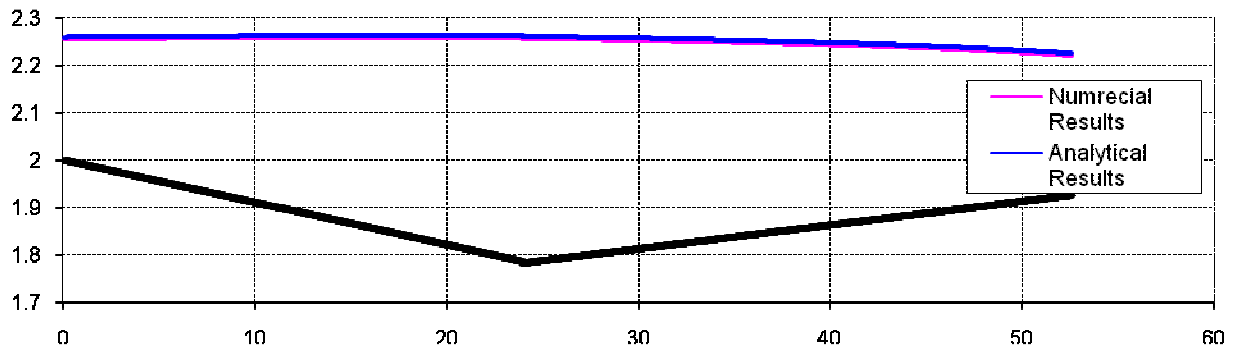


Figure 4. Water depth profile along the centerline of the channel for mild and inverse bed slopes

The third test is a challenging test which contains an inverse slope ( $S_0=-0.01$ ) followed by a steep slope ( $S_0=0.02$ ). The inflow discharge is reported as  $Q=0.16m^3/s$  [5] using both of third and fourth method of bed slope simulation while the fourth and third terms utilized in first and second parts of the channel, respectively. In this test, the inverse slope provides sub-critical flow along the first part and after forming the critical depth super-critical flow is developed in the second part with the steep slope. Hence, the flow is mixed of sub and super-critical flow. Note that in this test, in the initial conditions assumed the flow is super-critical at the entire channel. According to the flow regime, at the upstream boundary, the flow is sub-critical and free stream velocity components (unique width discharge) imposed while the depth extrapolated from the interior point. At the downstream boundary, the flow is super-critical and the free stream velocity components and depth extrapolated from the interior points. Therefore, in this test the water depth is not imposed at any flow boundary. The critical depth computationally forms where the flow regime changes (at the position of changing the bed slope). The computed flow depth develops toward up-stream as well as down-stream from this internal boundary. Due to inverse slope increased water depth and A2 profile is formed at the first part of the channel (Fig. 5). At the second part of the channel sub-critical flow is changed to super-critical flow and S2 profile is developed (Fig. 5). As it can be seen in the figure 5, the computed critical depth appeared at the beginning of the second part of the channel.

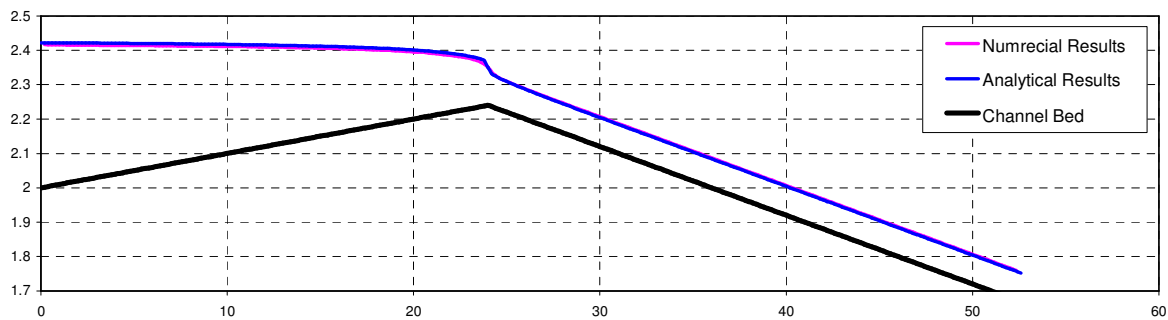


Figure 5. Water depth profile along the centerline of the channel for inverse and steep bed slopes

## Conclusion

Using depth averaged equations of continuity and motions, two-dimensional free surface flow in dual slope channels are simulated. The cell vertex finite volume method on triangular unstructured mesh is used to discretize the governing equations. In present work, the effect of bed slope is modeled by considering the bed elevation in the gravitational term of the equations of motions. The numerical oscillations due to explicit procedure of computations are damped out by application of the bi-harmonic artificial dissipation formulation suitable for the unstructured triangular meshes. The numerical model works with 2D triangular unstructured meshes, which represent 3D characteristics using the bed elevation at each nodal point.

The developed model was applied for simulating free surface flows in a long channel with two different bed slopes. Three conditions of dual slopes, which produce sub-critical, super-critical, and mixed flow regimes, were examined. The cases include the conditions that water surface does not follow the bed slope direction. Moreover, the situation that critical depth should form computationally in the flow domain is successfully tested.



Proper initial and flow boundary conditions were implemented and the complicated bed slope conditions were successfully simulated with small increase in computational effort

## References

1. Vreugdenhil, C.B., 1994, "Numerical Methods for Shallow Water Flow", Kluwer Academic Publisher
2. Abbot, A.B. 1980, Computational Hydraulics, Pitman Publishing Limited
3. Unami, K., Kawachi T., Babar M. & Itagaki H., "Two-Dimensional Numerical Model of Spillway Flow", Journal of Hydraulic Engineering, ASCE, Vol. 125, 1999, No. 4, PP. 369-375
4. Sabbagh-Yazdi S.R. & Mohamad Zadeh Qomi, M., "Using 2D Unstructured Mesh for Numerical Simulation of Free Surface Flow in Meandering Canal", Proceeding of Shallow Flow, TU Delft, Netherlands, 2003.
5. Zhou, J.G., 1995, Velocity-Depth Coupling in Shallow-Water Flows, Journal of Hydraulic Engineering, Vol.121, No.10, PP. 717-724
6. Thompson Joe F. & Soni, Bharat K. & Weatherill, Nigel P., 1999, "Hand book of grid generation", CRC Press
7. Jameson, A, Schmidt, W. & Turkel E., Numerical Solution of the Euler Equations by Finite Volume Method Using Runge – Kutta Time Stepping Schemes, AIAA Paper, 81-1259, June 1981
8. Chaudhry, M. H. & Younus M., "A Depth Averaged k- $\epsilon$  Turbulence Model for the Computation of Free Surface Flow", Journal of Hydraulic Research, Vol. 32, 1994, No.3, PP. 415-444
9. Weatherill, N.P. & Hassan ,O. & Marcum D.L., Calculation of Steady Compressible Flow-Fields with the Finite Elements Method, 31 Aerospace Sciences Meeting and Exhibit, 1993, AIAA-93-0341
10. Enander, R. & Karlsson, A.R., Implicit Explicit Residual Smoothing in Multi-grid Cycle, 33<sup>rd</sup> Aerospace Sciences Meeting and Exhibit, 1995, AIAA 95-0204
11. Sabbagh-Yazdi S.R., "Simulation at the Incompressible Flow Using the Artificial Compressibility Method", Ph.D. Thesis, University of Wales, Swansea, 1997.